Experimental Study of Double-Pulse Laser Micro Sintering: A Novel Laser Micro Sintering Process

Hanyu Song, Zheng Kang, Ze Liu and Benxin Wu*

School of Mechanical Engineering, Purdue University, West Lafayette, IN 47907, USA

Abstract: In laser micro sintering (LMS), good densification and low porosity of sintered material is often desirable for good mechanical properties. Recently, a novel LMS process, with the name of "double-pulse laser micro sintering" (DP-LMS), was proposed by the corresponding author. DP-LMS utilizes laser pulse group(s) consisting of "sintering laser pulse(s)" followed by "pressing laser pulse(s)" at a suitable delay time. This reported work has *preliminarily* demonstrated that, under the studied conditions, DP-LMS can produce an improved sintering result than those by LMS under similar conditions without using the "double-pulse" approach. The potential underlying mechanism has been discussed.

Keywords: laser sintering; laser micro sintering

1. Introduction

Laser sintering, in a broad sense, is a process of converting powder particles into a more continuous medium through coalition of particles under laser irradiation (the process is often called "laser melting" when full melting of particles occurs) [1, 2]. Laser sintering can be used in areas such as flexible electronics fabrication, composites fabrication or the rapid and flexible additive manufacturing of parts [3-6]. When laser sintering is used to produce parts with micro-scale features, the process can be called laser micro sintering (LMS) [7-12], during which pulsed lasers are often used [7-10].

The mechanical properties of sintered material often strongly depend on the material densification and porosity [13]. Hence, in LMS good densification and low porosity are often desirable in order to manufacture parts with good mechanical properties. A novel LMS process, called "double-pulse laser micro sintering" (DP-LMS), was recently proposed by the

* Corresponding author: Benxin Wu, Associate Professor, School of Mechanical Engineering, Purdue University, 585 Purdue Mall, West Lafayette, IN 47907, USA, email: wu65@purdue.edu

corresponding author [14] (and such a kind of LMS process has been rarely reported in the literature to the authors' best knowledge). This paper reports experimental work, which has *preliminarily* demonstrated that, under the studied conditions, the novel DP-LMS process can produce an improved sintering result (i.e., an apparently more continuous and densified sintered region on an optical micrograph shown later in this paper) compared with those by laser micro sintering processes under similar conditions without using the "double-pulse" approach. The potential underlying physical mechanism for DP-LMS will also be discussed.

The major goal of this reported work is to preliminarily confirm the potential advantages of the DP-LMS process. Hence, only a single surface layer in a small region of a powder target is sintered, and the sintering results are mainly assessed based on optical microscopic images. Lots of further work is certainly still needed on the novel DP-LMS process.

2. The DP-LMS Process and Experimental Setup

As shown in Fig. 1, during DP-LMS, the sintering process is carried out using one or multiple groups of laser pulses, where each group comprises N_1 "sintering laser pulses" followed by N_2 "pressing laser pulses" at a suitable delay time τ_0 (where N_1 and N_2 are integers equal to or larger than 1). The "sintering laser pulses" are fired to "sinter" the target powder particles (i.e., coalesce the particles into a more continuous medium), while the "pressing laser pulses" are used to promote the material densification and reduce porosity through laser-induced high pressure onto the material surface (the related potential mechanism will be discussed in more details later). Although the novel process is called "*double-pulse* laser micro sintering", each laser pulse group may have *more than two pulses* (i.e., the sum of N_1 and N_2 could be larger than 2).

There are various possible ways of carrying out the DP-LMS process. For the study reported in this paper, the values of N_1 and N_2 are chosen to be 10 and 1, respectively. The schematic of the experimental setup is shown in Fig. 2a. In each laser pulse group, the "sintering pulses" generated by Laser A (SPI G3.0) are effectively mainly 10 pulses, each of which has a total pulse duration of ~200 ns and a wavelength of ~1064 nm. The average sintering pulse energy in each laser pulse group is ~0.09 mJ/pulse. The distance in time between two neighboring sintering pulses in the same laser pulse group is ~40 µs. The "pressing pulse" has a full-width-at-half-maximum duration of ~5 ns (which also has a wavelength of ~1064 nm), a pulse energy of ~0.22 mJ/pulse, and is generated from Laser B (Bright Solutions, Onda). In each laser pulse group, the distance in time between the rising edge of the last "sintering pulse" and the peak of the "pressing pulse" is τ_0 , which is controlled using a digital delay generator (Berkeley Nucleonics, Model 577). The laser beams are delivered to the target surface using a scan head (ScanLab, HurryScan 14), which contains mirrors and a focusing lens with f = 100 mm. The target (cobalt powder supported by an aluminum substrate) is positioned by XYZ motion stages (not drawn in Fig.2a) at a certain location below the scan head. The laser pulse energies given in this paper are the ones measured after laser beam propagates through the scan head. The laser spot diameter at the target surface has been estimated based on the knife-edge method (and the approximate assumption that the laser intensity in the spot follows a Gaussian distribution) to be roughly ~70 µm and ~115 µm for the sintering pulse and the pressing pulse, respectively. The two laser spots are approximately concentric, and the concentricity is expected to be sufficient for the purpose of this study. The sintering experiments are performed in ambient air.

The cobalt powder (Alfa Aesar, Product number: 10455) used in this work has a nominal size of ~1.6 micron listed in the product specification. The powder is put into 95% ethanol and treated by a magnetic stirrer for about 15 minutes to create a cobalt suspension. Then, a pipette is employed to deposit multiple drops of the suspension into the ~1 cm × 1 cm slot surrounded by ~0.5 mm thick aluminum slices placed on an aluminum substrate, as shown in Fig.2b. After the deposited suspension is completely dry, excessive cobalt powder that is higher than the aluminum slice surface is removed using a knife blade. Then, the thin aluminum slices are removed, leaving a layer of cobalt powder onto the aluminum substrate, which is then used as the target in the sintering experiments.

To sinter a surface region of the target that is larger than the laser spots at the target surface, multiple surface locations (as shown in Fig. 2c) are laser-irradiated. For each of the 9 (= 3 × 3) locations, one laser pulse group is sent, which consists of 10 "sintering pulses" followed by 1 "pressing pulse" as introduced earlier. Laser spots are stationary during the irradiation of one surface location. Then the laser spots will be moved to the next location using motion stages, after which the next laser pulse group is sent to the location. The center-to-center distance between adjacent locations is ~75 μm as shown in Fig.2c. After sintering, the sintered surface region is observed using an optical microscope. As comparisons to the DP-LMS process, sintering processes are also carried out without using the "double-pulse" approach (e.g., without using either the "pressing pulse" or the "sintering pulses" in each laser pulse group).

3. Results and Discussions

Figure 3a shows the optical microscopic image for the sintered surface-layer region of the cobalt powder target through the DP-LMS process (where, as introduced earlier, each of the 3×3 target surface locations is irradiated by a laser pulse group, which consists of 10 "sintering pulses" (~0.09 mJ/pulse on average) followed by 1 "pressing pulse" of ~0.22 mJ at a delay time of $\tau_0 =$

$\sim 700\ ns$). As a comparison, Fig. 3b shows the image for the surface region sintered in a similar way, but without using the “pressing pulse” for each irradiated surface location (i.e., each surface location is irradiated only by the 10 “sintering pulses”). In Fig. 3b, the laser-sintered surface region does not appear very continuous and densified. Instead, an obvious “balling” phenomenon is observed, and many small sphere-like structures are formed after the melting and re-solidification of some powder particles. On the other hand, in Fig. 3a the surface region sintered by the DP-LMS process appears much more continuous and densified with a much less severe balling phenomenon than that in Fig. 3b. A natural question will be: is this simply due to the larger total laser energy irradiated onto each target surface location for Fig. 3a than that for Fig. 3b?

Figure 3c and 3d show the images for the surface regions sintered in a way similar to Fig.3b, except that: (i) for Fig. 3c the number of sintering pulses in each laser pulse group is increased by 10, and (ii) for Fig. 3d, the average pulse energy of the sintering pulses in each laser pulse group is increased from ~0.09 mJ/pulse to ~0.13 mJ/pulse. No “pressing pulse” is used for Fig. 3c and 3d. The total laser energy irradiated onto each target location in Fig. 3c or 3d is larger than that for Fig. 3a (the DP-LMS situation). However, the laser-sintered surface regions in Fig. 3c and 3d still do not appear very continuous and densified, and a severe “balling” phenomenon still exists. This provides supporting evidence that the better sintering result that appears in Fig. 3a for DP-LMS is unlikely simply due to more laser energy input at each irradiated target surface location.

Figure 3e shows an image for the powder target surface region treated by sending 5 “pressing laser pulses” (at ~0.22 mJ/pulse on average and with a pulse-to-pulse separation time of ~40 μs) to each of the irradiated 3×3 target surface locations without sending any “sintering laser pulse". It can be seen that the laser pulses have induced obvious material removal from the target and left multiple "holes" on the target surface.

Figure 3f shows an image for the surface region sintered by the DP-LMS process under a condition similar to that for Fig. 3a, except with a much larger sintering-pressing pulse separation time in each laser pulse group (τ_0 = ~1 ms). The sintered surface region under τ_0 = ~1 ms in Fig. 3f appears to be less continuous, densified, and shows a more severe "balling" phenomenon than that in Fig.3a under τ_0 = ~700 ns. The results suggest that under the conditions investigated, the delay time τ_0 during DP-LMS needs to be properly selected to produce good sintering results.

The exact underlying mechanisms involved in the novel DP-LMS process still require further work to fully understand. One important mechanism likely involved is expected to be the following (see Fig.4 for a schematic): for each laser pulse group, after the last "sintering laser pulse" is fired, laser-induced target powder melt may still exist when the following "pressing laser pulse" comes. The "pressing laser pulse" can induce material removal (through vaporization and/or other mechanism(s)) from the irradiated target surface, and even generate high-pressure plasma plume at or near the surface when the laser intensity is sufficiently high; as a result, a high-pressure pulse can be generated onto the target material surface [7, 15, 16]. The high pressure may promote the melt flow and/or press the target material, which could reduce the "balling" effect, decrease the porosity and/or promote the densification of sintered material. Further work is still needed to confirm the aforementioned mechanism and fully understand the DP-LMS process.

During DP-LMS, the parameters of the "sintering laser pulse(s)" and "pressing laser pulse(s)" can be selected *independently*, which can potentially give a good process adjustability and flexibility. The sintering and pressing laser pulse parameters can be optimized for the main purposes of sintering and "pressing" (i.e., generating high pressure), respectively. Target powder melt may possibly exist for quite some additional time after the last "sintering laser pulse" ends, and the effects of high-pressure impact onto the target material at different timings could be different. The relatively best result can be potentially achieved by sending suitable "pressing laser pulse(s)" at the most suitable timing(s). To produce a high pressure without causing excessive target material removal, the "pressing laser pulse(s)" may often be desired to have a sufficiently high intensity (W/m^2), sufficiently low total fluence (J/m^2), and hence a relatively short pulse duration. A sufficiently low total fluence may be desired because the amount of target material removed per unit (irradiated) surface area by the "pressing pulse(s)" is often proportional (although not necessarily linearly and not necessarily always) to the total fluence. In addition, because the eventual goal of DP-LMS is to sinter material, when laser parameters are selected typically the following requirement needs to be satisfied: each laser pulse group can effectively induce material sintering and the amount of material sintered should be larger than the amount of material removed or ablated. The laser parameters selected and employed in this study, including the values of N_1 and N_2 and the laser beam profile, are certainly not necessarily the only possible choices for DP-LMS.

4. Conclusions

This paper reports preliminary study on a novel DP-LMS process that was proposed recently by the corresponding author [14]. During the studied DP-LMS process, as introduced earlier target powder particles are sintered by a laser pulse group that consists of 10 "sintering pulses" followed by 1 "pressing pulse" at each laser-irradiated target location. Optical microscopic images show that under the conditions studied, the surface region sintered by the novel DP-LMS process with a suitable delay time τ_0 appears to be more continuous, densified, and/or have a less severe balling phenomenon in the image than those sintered by: (1) using only the "sintering pulses" with the same pulse energy and number as those in DP-LMS for each laser-irradiated location; (2) using only the "sintering pulses", but with a larger pulse energy or pulse number; and (3) using only multiple "pressing pulses". This study shows a great potential of the novel DP-LMS process, while further research work is still needed to confirm and better understand its capability, performance and fundamental mechanisms.

Acknowledgment and Declaration of Interest

This material is based upon work supported by the National Science Foundation under Grant No. CMMI 1728481. A provisional patent application on DP-LMS was filed [14], for which the corresponding author is the inventor (who received no related royalties by the time the manuscript was submitted).

List of References

1. Kruth, J.P., Mercelis, P., Van Vaerenbergh, J., Froyen, L., Rombouts, M., “Binding mechanisms in selective laser sintering and selective laser melting”, Rapid Prototyping Journal, 11: 26-36, 2005.
2. Wang, Y., Shi, J., Lu, S. and Wang, Y., “Selective laser melting of graphene-reinforced Inconel 718 superalloy: evaluation of microstructure and tensile performance”, Journal of Manufacturing Science and Engineering, 139: 041005, 2017.
3. Ko, S. H., Pan, H., Grigoropoulos, C. P., Luscombe, C. K., Fréchet, J. M. J., Poulikakos, D., “All-inkjet-printed flexible electronics fabrication on a polymer substrate by low-temperature high-resolution selective laser sintering of metal nanoparticles”, Nanotechnology, 18: 345202, 2007.
4. Guo, N., Leu, M.C., “Additive manufacturing: technology, applications and research needs”, Frontiers of Mechanical Engineering, 8: 215–243, 2013.
5. Gittard, S.D., Narayan, R.J., “Laser direct writing of micro- and nano-scale medical devices”, Expert Review of Medical Devices, 7:343–356, 2010.
6. Lin, D., Liu, C.R., Cheng, G.J., "Laser sintering of separated and uniformly distributed multiwall carbon nanotubes integrated iron nanocomposites." Journal of Applied Physics 115: 113513, 2014.
7. Regenfuss, P., Streek, A., Hartwig, L., Klötzer, S., Brabant, Th., Horn, M., Ebert, R., Exner, H., "Principles of laser micro sintering", Rapid Prototyping Journal, 13:204-212, 2007.
8. Streek, A., Regenfuss, P., Exner, H., "Fundamentals of energy conversion and dissipation in powder layers during laser micro sintering", Physics Procedia, 41:851–862, 2013.
9. Zhu, H., Ke, L., Lei, W., Dai, C., Chen, B., "Effect of the Q-switch parameters on the sintering behavior of laser micro sintering Cu-based metal powder using Q-switched Nd-YAG laser." Rapid Prototyping Journal, 19: 44-50, 2013.
10. Ke, L., Zhu, H., Yin, J., Wang, X., "Effects of peak laser power on laser micro sintering of nickel powder by pulsed Nd: YAG laser." Rapid Prototyping Journal, 20: 328-335, 2014.
11. Streek, A., Regenfuss, P., Ebert, R., Exner, H., "Laser micro sintering–a quality leap through improvement of powder packing", in The Proceedings of the 19th Annual SFF Symposium, vol. 297, 2008.
12. Vaezi, M., Seitz, H., Yang, S., "A review on 3D micro-additive manufacturing technologies", The International Journal of Advanced Manufacturing Technology, 67:1721-1754, 2013.
13. Li, L., Aubertin, M., “A general relationship between porosity and uniaxial strength of engineering materials”, Canadian Journal of Civil Engineering, 30: 644-658, 2003.
14. US provisional patent application, “Double-pulse laser micro sintering”, Inventor: Benxin Wu; Application number: 62693684, Receipt date: 07/03/2018.
15. Harilal, S.S., Miloshevsky, G.V., Diwakar, P.K., LaHaye, N.L., Hassanein, A., "Experimental and computational study of complex shockwave dynamics in laser ablation plumes in argon atmosphere", Physics of Plasmas, 19:083504, 2012.

16. Tao, S., Zhou, Y., Wu, B., Gao, Y., "Infrared long nanosecond laser pulse ablation of silicon: integrated two-dimensional modeling and time-resolved experimental study", Applied Surface Science, 258:7766–7773, 2012.

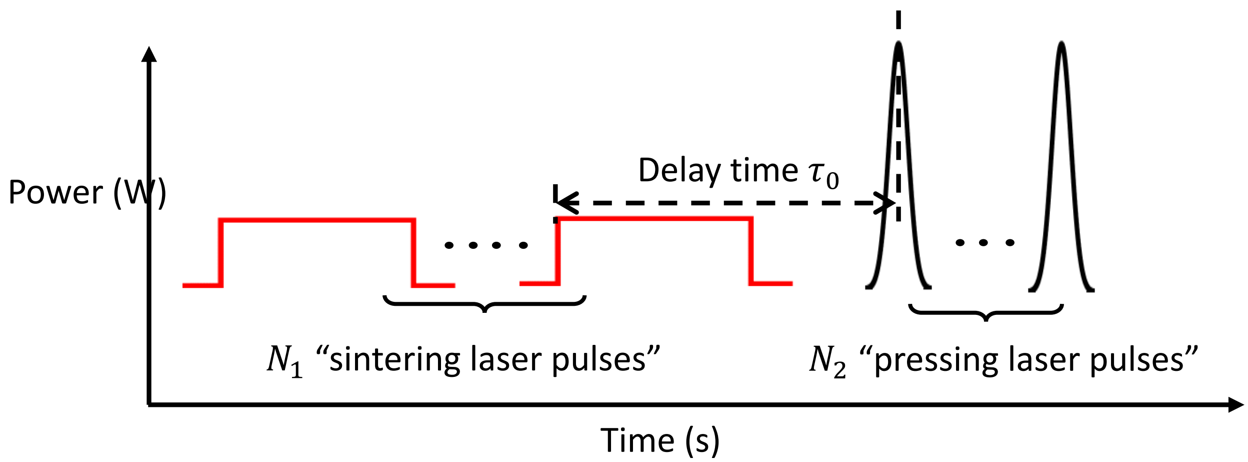

Figure 1. Schematic diagram demonstrating the general concept of laser pulse format in each laser pulse group for the novel double-pulse laser micro sintering (DP-LMS) process (the schematic is not drawn to scale; and it does not necessarily include all the actual components, details and/or denote them in an exact way).

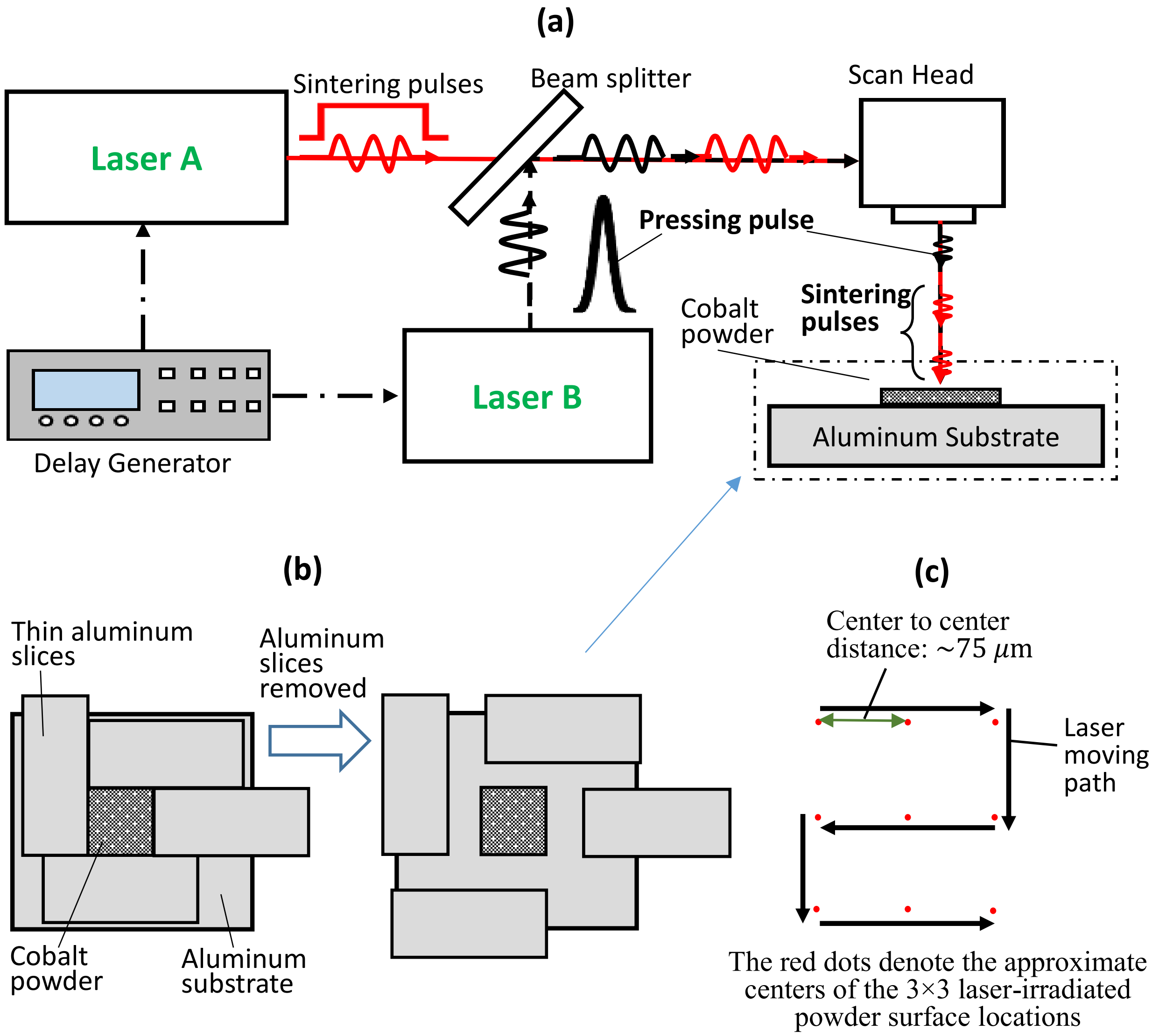

Figure 2. Schematics of: (a) the experimental setup of the double-pulse laser micro sintering (DP-LMS) process in this study (not all components are shown); (b) the preparation process of the target (a cobalt powder layer supported by an aluminum substrate); and (c) laser-irradiated 3 × 3 powder surface locations during laser sintering (all the schematics are typically not drawn to scale; and they do not necessarily include all the actual components, details and/or denote them in an exact way).

(a) DP-LMS, $\boldsymbol{\tau_0 = \sim 700\, ns}$,
10 sintering pulses (~0.09 mJ/pulse) **+ 1 pressing pulse** (~0.22 mJ/pulse) for each of the 3×3 laser-irradiated locations

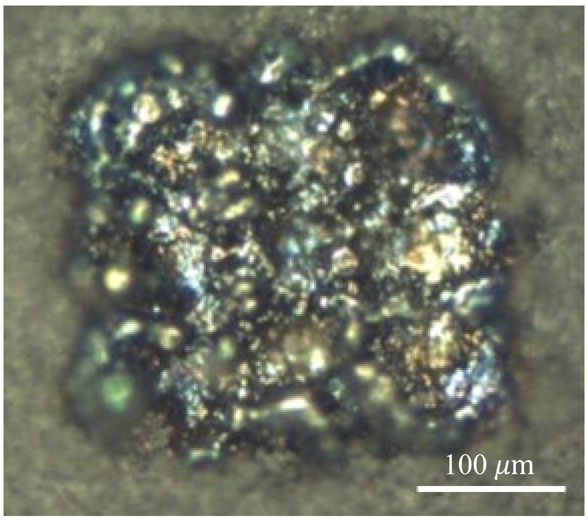

(b) 10 sintering pulses only for each laser-irradiated location (~0.09 mJ/pulse)

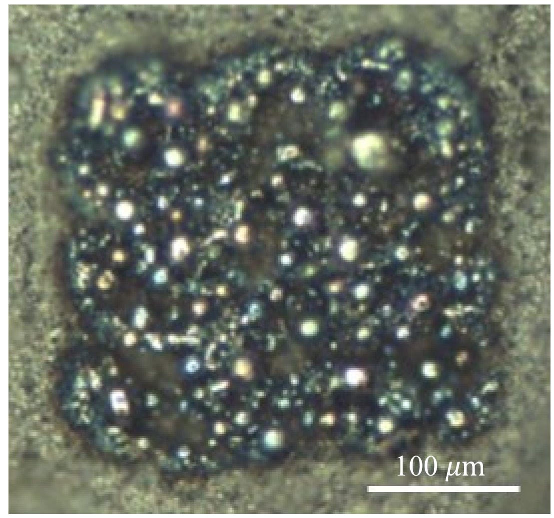

(c) 20 sintering pulses only for each laser-irradiated location (~0.09 mJ/pulse)

(d) 10 sintering pulses only for each laser-irradiated location (~0.13 mJ/pulse)

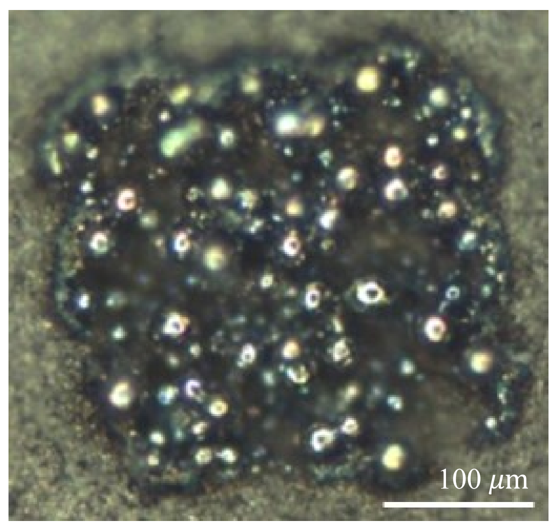

(Figure 3 continues on the next page)

(e) 5 pressing pulses only for each laser-irradiated location (~0.22 mJ/pulse)

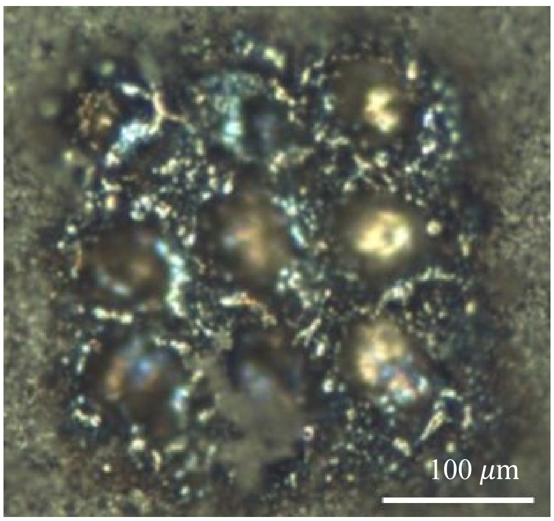

(f) DP-LMS, under conditions similar to (a), except $\boldsymbol{\tau_0 = \sim 1\ ms}$

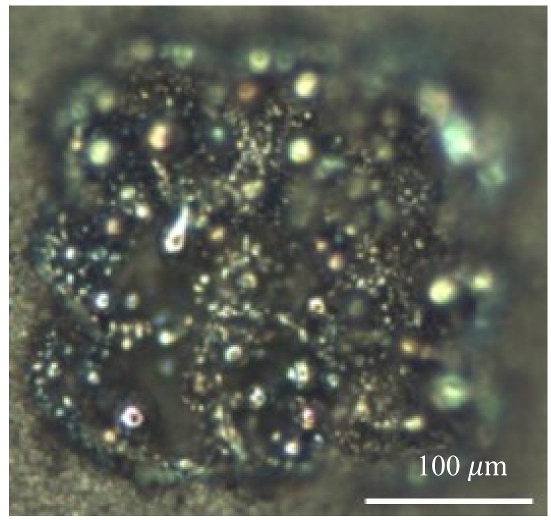

Figure 3. Optical microscopic images of target surface regions sintered by: (a) DP-LMS, with τ_0= ~700 ns, 10 sintering pulses (~0.09 mJ/pulse) + 1 pressing pulse (~0.22 mJ/pulse) for each of the laser-irradiated 3 × 3 surface locations; (b) 10 sintering pulses only for each location (~0.09 mJ/pulse); (c) 20 sintering pulses only for each location (~0.09 mJ/pulse); (d) 10 sintering pulses only for each location (~0.13 mJ/pulse); (e) 5 pressing pulses only for each location (~0.22 mJ/pulse); and (f) DP-LMS under conditions similar to (a) except τ_0= ~1 ms.

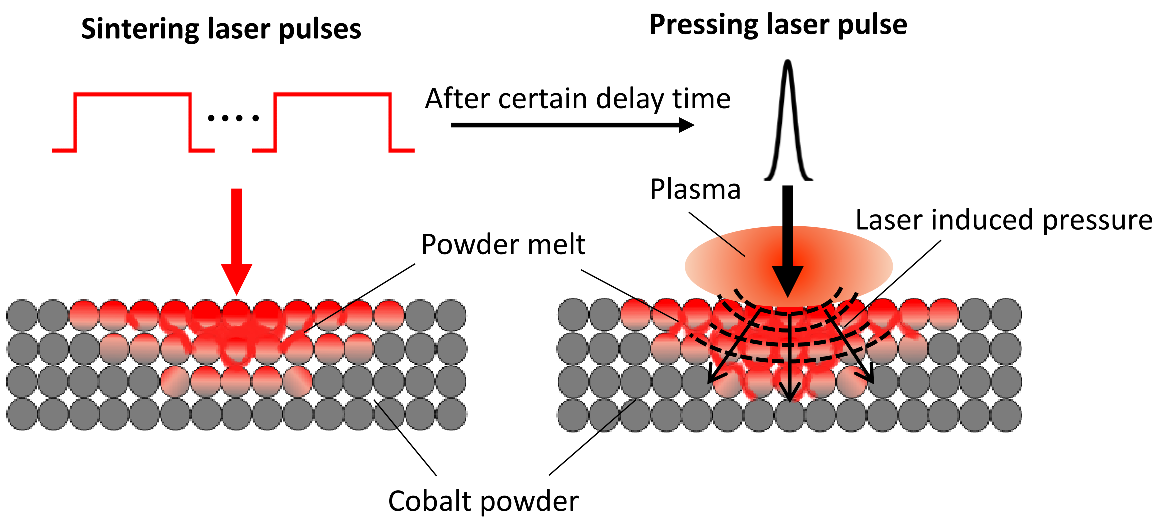

Figure 4. Schematic for a possible fundamental mechanism of the DP-LMS process (the schematic is not drawn to scale, does not necessarily include all the actual components, details and/or denote them in an exact way).

.